doi:10.1246/cl.2012.792
Published on the web July 28, 2012

Carburized, Lithium-doped Ni/ZrO_2 for Preventing CO_2 Conversion during CO Methanation

Masatoshi Nagai* and Shinpei Yamashita
Graduate School of Bio-applications and Systems Engineering, Tokyo University of Agriculture and Technology, Koganei, Tokyo 184-8588

(Received April 5, 2012; CL-120298; E-mail: mnagai@cc.tuat.ac.jp)

Doping 20 wt % Ni/ZrO_2 with 0.1 and 1.0 wt % Li prevented the adsorption and methanation of CO_2 and promoted the methanation of CO. Lithium-doped NiC formed the active site in the catalyst. Carburized undoped Ni/ZrO_2, Cs-doped Ni/ZrO_2, and reduced Li-doped Ni/ZrO_2 catalysts did not prevent CO_2 methanation.

Fuel cells are among several energy conversion devices that are the subject of intense interest for solving energy resource problems. Fuel cells are currently costly, because of their complex structure; they require a reforming unit that produces hydrogen from natural gas or oil. To reduce CO at approximately 1 vol % in the reformate, the remaining CO must be methanated faster than the preferential oxidation of CO. The methanation of CO in the absence of CO_2 has been investigated in metal-doped Ni/Al_2O_3,[1,2] Ni/MCM-41,[3] and group 8 metal catalysts.[4] Regarding the support, zirconia is used for Ni and titania is used for Ru, because Ni particles are large and Ru particles are small.[5,6] The methanation of CO accompanies that of the CO_2 contained in the reformate, which leads to an increase in hydrogen consumption. Therefore, the catalyst must be selective for CO methanation over CO_2 methanation and must not consume hydrogen. Several metal-doped Ru/TiO_2 and Ru/Al_2O_3 catalysts[7–9] selectively promote CO methanation. In addition, Re-doped Ni/ZrO_2[10] decreases the undesired CO_2 methanation and maintains the CO methanation. Adsorbed CO_2 dissociates to form adsorbed CO and O species, and the subsequent reaction of the adsorbed CO to form CH_4 has been examined. Methanation of CO mainly occurs at the Ni metal sites, where CO_2 dissociation is suppressed by the addition of Ru, which significantly improves selective CO methanation.[11] However, a catalyst is required to effectively reduce CO in the temperature range where CO_2 does not react. A highly selective Ru-doped Ni/Al_2O_3 catalyst has been used to methanate CO and to block the adsorption of CO_2.[12,13] Nickel is an effective support for CO_2 methanation catalysts that do not contain Ru or noble metals. Ni/TiO_2 is more active than Ni/Al_2O_3, Co/TiO_2, and Fe/TiO_2.[14]

Transition-metal carbides, such as nickel molybdenum and nickel carbides, promote the dissociation of water in the water–gas shift reaction and ethanol steam reforming.[15,16] Moreover, ZrO_2 protects against the oxidation of carbides and promotes the exchange of the lattice oxygen with the oxygen atom of the dissociated water,[17] which in turn prevents the catalyst from becoming deactivated. Thus, carburized nickel on zirconia is a promising alternative to ruthenium. Furthermore, Cs-doped Ni/ZrO_2 efficiently promotes the water–gas shift reaction for hydrogen production, even in the presence of CO_2.[18] However, alkali-metal-doped catalysts are needed that promote H_2O dissociation and prevent H_2 consumption and CO_2 methanation. The catalyst must selectively methanate CO with no CO_2 dissociation.

We have carburized Ni/ZrO_2 doped with Li to prevent the methanation of CO_2. The Li-doped carburized Ni/ZrO_2 increased the formation of NiC and prevented the dissociation of CO_2.

The Ni catalysts were prepared by impregnating the ZrO_2 support with Ni; an Al_2O_3-supported catalyst was also prepared for comparison. An aqueous solution of $Ni(NO_3)_2 \cdot 6H_2O$ was used to introduce NiO (20 wt %) onto the support, which was then oxidized at 500 °C in air. An aqueous solution of $LiNO_3$ or $CsNO_3$ was added gradually to the oxidized precursor containing Ni and the support, and the mixture was dried at 120 °C and calcined at 500 °C for 5 h in air. The precursor (0.2 g) was carburized from 450 to 550 °C in a stream of 20% CH_4/H_2 at the rate of 60 °C h^{-1}; the temperature was maintained at 550 °C for 2 h and then cooled to room temperature. The carburized catalyst was then used for methanation or analysis without exposure to air. The methanation activity was measured at 230 and 250 °C in a stream of 1.0% CO, 20% CO_2, 15% H_2O, and 64% H_2 in a He balance gas at a flow rate of 3.6 L h^{-1}, and with ultrapure water at the rate of 0.3 mL h^{-1}. The feed and reaction products were quantitatively analyzed by using an online gas chromatograph. The carburized Ni catalysts were characterized by Brunauer–Emmett–Teller (BET) surface area analysis, X-ray diffraction (XRD), transmission electron microscopy (TEM), and X-ray photoelectron spectroscopy (XPS). The effect of the Li doping on the surface properties of the Ni/ZrO_2 catalyst was determined by temperature-programmed desorption (TPD). For the TPD measurements, the catalyst was heated from room temperature to 900 °C at a rate of 10 °C min^{-1} in a 0.9 L h^{-1} stream of He, and CO_2 was added to the Li-doped and undoped Ni/ZrO_2 catalysts in a stream of He at 100 °C. CO_2 ($m/z = 44$) was monitored by using a quadruple mass spectrometer.

The XRD patterns confirmed the formation of metallic Ni and NiC in the Li-doped and undoped Ni/ZrO_2, carburized in 20% CH_4/H_2 at 550 °C (Figure 1). The carburized catalysts contained NiC ($2\theta = 44.4$ and 75.4°; PDF#14-0020) and metallic Ni ($2\theta = 44.5$ and 76.4°; PDF#87-0712), and NiO ($2\theta = 37.3°$) and Ni_3C were not observed.[19,20] In contrast, the XRD analysis showed that the carburized Li-doped and undoped Ni/Al_2O_3 contained metallic Ni and NiO ($2\theta = 37.3$, 43.4, and 75.6°; PDF#75-0197) but no NiC. Although the metallic Ni peak overlap with that of NiO at $2\theta = 37.3°$, these peaks were separate from those of metallic Ni and NiC in the case of carburization, and metallic Ni and NiO in the case of reduction. The NiC peaks were observed after the reaction, indicating the stability of nickel carbide during the reaction.

To examine the effect of Li doping on the surface composition of metallic Ni and NiC, the XPS C1s peak of the

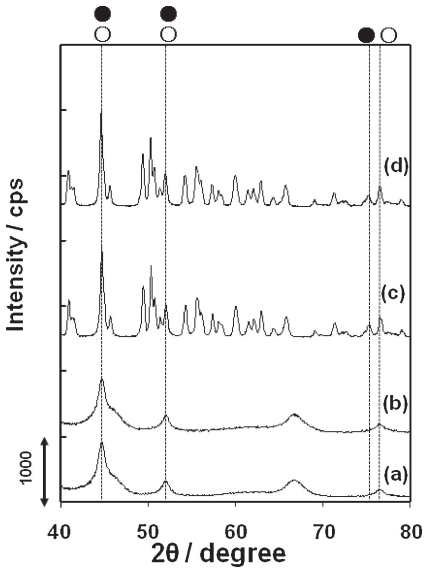

Figure 1. XRD patterns for (a) undoped and (b) Li-doped Ni/Al_2O_3 and (c) undoped and (d) Li-doped Ni/ZrO_2. ●: NiC; ○: Ni metal

Table 1. The ratio of carbidic to graphitic carbon calculated from the XPS 1s binding energy for Li-doped and undoped Ni/ZrO_2 carburized at 550 °C

	Ni/Zr	C/Zr	Carbon total /Ni	Carbidic /graphitic carbon
$NiLi/ZrO_2$	1.096	3.33	3.04	0.588
Ni/ZrO_2	0.828	6.12	7.40	0.488

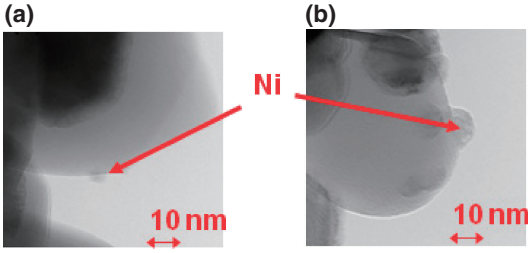

Figure 2. TEM images for (a) Li-doped and (b) undoped Ni/ZrO_2.

1% Li-doped and undoped Ni/ZrO_2 catalysts was determined (Table 1). The Li-doped Ni/ZrO_2 had a higher Ni/Zr ratio but a lower C/Zr ratio than the undoped Ni/ZrO_2, indicating that the Li doping brought Ni to the surface and reduced carbon deposition. Moreover, the ratio of carbide to graphite carbon for the Li-doped Ni/ZrO_2 was higher than that for the undoped Ni/ZrO_2. This indicates that the Li-doped Ni/ZrO_2 had 1.2-fold more carbide carbon than the undoped Ni/ZrO_2.

The TEM images of the Li-doped and undoped Ni/ZrO_2 catalysts are shown in Figure 2. A small Ni particle, approximately 5 nm in diameter, was visible on a large ZrO_2 particle in the Li-doped Ni/ZrO_2. In the undoped Ni/ZrO_2, a 12-nm-diameter Ni particle was visible on a ZrO_2 particle. This indicates that Li doping decreased the size of the Ni particles and that Ni was highly dispersed on the ZrO_2 in the Li-doped Ni/ZrO_2.

Table 2. Comparison of the CO and CO_2 conversion, H_2 consumed, and methane formation for Li-doped and undoped Ni/ZrO_2 and Ni/Al_2O_3 carburized at 550 °C

	CO Conv.	CO_2 Conv.	H_2 Consum.	Formed CH_4 /mmol g^{-1} min^{-1}
$NiLi/ZrO_2$	84.3[a] (82.9)[b]	0 (1.1)	10.6 (3.5)	0.172 (0.0911)
Ni/ZrO_2	75.4 (77.6)	4.9 (0)	21.1 (9.8)	0.151 (0.077)
$NiLi/Al_2O_3$	32.0 (0)	0.6 (0.1)	0 (0)	0.262 (0.0981)
Ni/Al_2O_3	31.1 (22.0)	2.4 (0)	9.2 (4.2)	0.031 (0.0692)

[a]Reaction temperature of 250 °C. [b]Reaction temperature of 230 °C.

The conversion of CO and CO_2 on the Li-doped and undoped Ni/ZrO_2 and Ni/Al_2O_3 at 230 and 250 °C is shown in Table 2. The conversion of CO on the Li-doped Ni/ZrO_2 catalyst was 82.9 and 84.3% at 230 and 250 °C respectively. In addition, the amount of hydrogen consumed was less than 11% and no significant CO_2 conversion was observed below 250 °C. The Li-doped and undoped Ni/Al_2O_3 catalysts were less active, and less selective during the CO methanation in the presence of CO_2, which suggests that the Li addition prevented the conversion of CO_2 to CH_4 and reduced the H_2 consumption. The BET surface areas of the Li-doped and undoped Ni/ZrO_2 were 5 and 6 $m^2 g^{-1}$, respectively, whereas the BET surface areas of the undoped and Li-doped Ni/Al_2O_3 were 203 and 210 $m^2 g^{-1}$, respectively. This result indicates that, despite having 1/20th the surface area of the Al_2O_3-supported catalyst, the ZrO_2-supported nickel catalyst was more active.

The methanation activity and selectivity of the nickel carbide and metallic Ni were evaluated. The Li-doped Ni/ZrO_2 carburized at 550 °C exhibited higher CO methanation activity and lower H_2 consumption (10.6%) than did the catalyst reduced at 550 °C (40%), as well as CO_2 conversion of 0% in contrast to the reduced catalyst, which had 5% CO_2 conversion at 250 °C. NiC selectively promoted CO methanation, whereas metallic Ni did not.

The 1.0 wt % Li-doped 20 wt % Ni/ZrO_2 was compared with the 1.0 and 10 wt % Cs-doped 20 wt % Ni/ZrO_2 catalyst at 250 °C (Figure 3). Li doping increased CO conversion and CH_4 formation and reduced H_2 consumption and CO_2 conversion. Therefore, the addition of 1.0 wt % Li prevented CO_2 conversion and promoted CO methanation. The same effect was also observed for 0.5 wt % Li-doped Ni/ZrO_2 (data not shown). In contrast, the 1.0 and 10 wt % Cs-doped catalyst did not display CO conversion and CH_4 formation, although it consumed H_2. Thus, the addition of Li prevented CO_2 methanation, whereas Cs prevented CO methanation. We have recently studied the steam reforming of ethanol on alkali-metal-doped Ni/ZrO_2 and reported that Cs-doped Ni/ZrO_2 increases hydrogen production more than Li-doped Ni/ZrO_2 does.[12] Cs doping promoted the C–H bond breaking through the CH_3CO species formed from CH_3CHO but not the C–O bond cleavage of CO and CO_2 during CO methanation.

To study the effect of Li, TPD was performed on the Li-doped and undoped Ni/ZrO_2 after injection of CO_2 into the stream of helium (Figure 4). A large CO_2 peak at 692 °C and small peaks at 471 and 534 °C were observed for Ni/ZrO_2, probably due to the three sites of CO_2 adsorption/desorption. However, Li doping blocked the main site for CO_2 adsorption

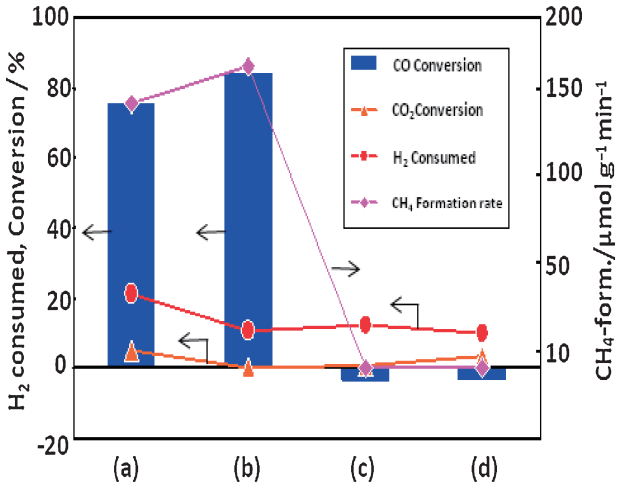

Figure 3. CO and CO_2 conversion, CH_4 formation rate, and H_2 consumption at 250 °C for carburized Ni/ZrO_2 that was (a) undoped and doped with (b) 1 wt % Li, (c) 1 wt % Cs, and (d) 10 wt % Cs.

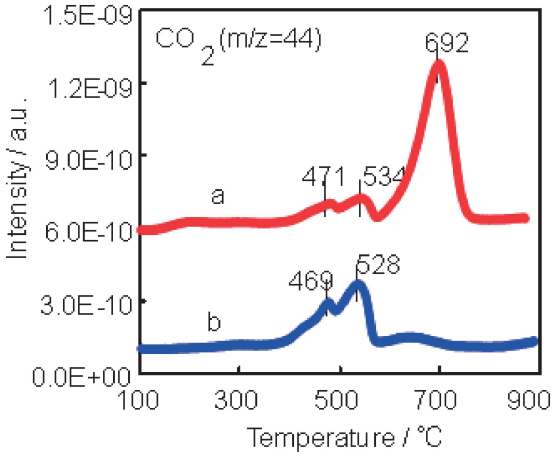

Figure 4. Temperature-programmed surface reaction desorption for 20 wt % Ni/ZrO_2 (a) with and (b) without 0.1 wt % Li in a stream of He after CO_2 adsorption.

which corresponded to the large peak. The XRD and XPS analyses suggest that the Li doping of Ni/ZrO_2 transformed the Ni metal on the catalyst surface into electron-rich NiC. The Li-doped Ni/ZrO_2 catalyzed selective CO methanation with no CO_2 methanation. The Ni metal on the Ni/ZrO_2 catalyzed the methanation of CO_2 and Li formed NiC from Ni metal.

In summary, Li-doped NiC catalyzed the methanation of CO and reduced hydrogen consumption, whereas undoped NiC catalyzed the methanation of both CO and CO_2.

References

1 K. O. Xavier, R. Sreekala, K. K. A. Rashid, K. K. M. Yusuff, B. Sen, *Catal. Today* **1999**, *49*, 17.
2 J. Chen, Y. Qiao, Y. Li, *Appl. Catal., A* **2008**, *337*, 148.
3 G. Du, S. Lim, Y. Yang, C. Wang, L. Pfefferle, G. L. Haller, *J. Catal.* **2007**, *249*, 370.
4 Y.-T. Tsai, J. G. Goodwin, Jr., *J. Catal.* **2011**, *281*, 128.
5 S. Takenaka, T. Shimizu, K. Otsuka, *Int. J. Hydrogen Energy* **2004**, *29*, 1065.
6 R. A. Dagle, Y. Wang, G.-G. Xia, J. J. Strohm, J. Holladay, D. R. Palo, *Appl. Catal., A* **2007**, *326*, 213.
7 M. B. I. Choudhury, S. Ahmed, M. A. Shalabi, T. Inui, *Appl. Catal., A* **2006**, *314*, 47.
8 S. Tada, R. Kikuchi, K. Urasaki, S. Satokawa, *Appl. Catal., A* **2011**, *404*, 149.
9 P. Panagiotopoulou, D. I. Kondarides, X. E. Verykios, *Appl. Catal., B* **2009**, *88*, 470.
10 M. Krämer, K. Stöwe, M. Duisberg, F. Müller, M. Reiser, S. Sticher, W. F. Maier, *Appl. Catal., A* **2009**, *369*, 42.
11 M. Kimura, T. Miyao, S. Komori, A. Chen, K. Higashiyama, H. Yamashita, M. Watanabe, *Appl. Catal., A* **2010**, *379*, 182.
12 A. Chen, T. Miyao, K. Higashiyama, H. Yamashita, M. Watanabe, *Angew. Chem., Int. Ed.* **2010**, *49*, 9895.
13 S. Komori, A. Chen, T. Miyao, K. Higashiyama, H. Yamashita, M. Watanabe, *J. Jpn. Pet. Inst.* **2011**, *54*, 50.
14 K. Urasaki, Y. Tanpo, T. Takahiro, J. Christopher, R. Kikuchi, T. Kojima, S. Satokawa, *Chem. Lett.* **2010**, *39*, 972.
15 Y. Miyamoto, M. Akiyama, M. Nagai, *Catal. Today* **2009**, *146*, 87.
16 M. Akiyama, Y. Oki, M. Nagai, *Catal. Today* **2012**, *181*, 4.
17 T. Namiki, S. Yamashita, H. Tominaga, M. Nagai, *Appl. Catal., A* **2011**, *398*, 155.
18 M. Nagai, A. M. Zahidul, Y. Kunisaki, Y. Aoki, *Appl. Catal., A* **2010**, *383*, 58.
19 Y. Leng, L. Xie, F. Liao, J. Zheng, X. Li, *Thermochim. Acta* **2008**, *473*, 14.
20 Y. Goto, K. Taniguchi, T. Omata, S. Otsuka-Yao-Matsuo, N. Ohashi, S. Ueda, H. Yoshikawa, Y. Yamashita, H. Oohashi, K. Kobayashi, *Chem. Mater.* **2008**, *20*, 4156.

